Electronic Supplementary Material (ESI) for Nanoscale.

Supporting Information

OER Process

The photocatalytic OER can be decomposed into four one-electron oxidation steps[1,2] releasing one proton and one electron at each step, as described below:

$$A: S_0 + H_2O \rightarrow S_1 + H^+ + e^- \quad (1)$$

$$B: S_1 \rightarrow S_2 + H^+ + e^- \quad (2)$$

$$C: S_2 + H_2O \rightarrow S_3 + H^+ + e^- \quad (3)$$

$$D: S_3 \rightarrow S_0 + O_2 + H^+ + e^- \quad (4)$$

, where S_0 denotes the bare surface and S_1, S_2 and S_3 denote the intermediate states of OER (i.e., adsorption of *OH, *O and *OOH, respectively). The Gibbs free energy change of each step from "A" to "D" under the influence of finite pH and potential bias U can be written as follows:

$$\Delta G_A = G_{S_1} + \frac{1}{2}G_{H_2} - G_{H_2O} - G_{S_0} - \Delta pH - eU_{ox} \quad (1)$$

$$\Delta G_B = G_{S_2} + \frac{1}{2}G_{H_2} - G_{S_1} - \Delta pH - eU_{ox} \quad (2)$$

$$\Delta G_C = G_{S_3} + \frac{1}{2}G_{H_2} - G_{H_2O} - G_{S_2} - \Delta pH - eU_{ox} \quad (3)$$

$$\Delta G_D = G_{S_0} + \frac{1}{2}G_{H_2} + G_{O_2} - G_{S_3} - \Delta pH - eU_{ox} \quad (4)$$

Here, the Gibbs free energy of $H^+ + e^-$ is replaced with $\frac{1}{2}G_{H_2}$ at the standard conditions of pressure and temperature. A correction of $\Delta pH = 0.0594 \times pH$ in OER at a specific pH condition is considered. Furthermore, an overall shift of Gibbs free

energy of eU_{ox} is imposed due to irradiation induced hole. U_{ox} is the hole potential in VBM relative to reduction potential of proton (H^+/H_2). The calculated Gibbs free energy of each species consists of three parts, including their electron energy, vibrational energy, and contribution of entropy. The calculated Gibbs free energy changes under the condition of U_{ox} = 0 eV are summarized in table S1.

Table S1. The Gibbs free energy changes (in the unit of eV) of each step involved in OER are calculated at the condition of pH =7 and U = 0 eV.

Sites	1	2	3	4
ΔG_A	1.985	2.015		1.156
ΔG_B	0.773	0.742		0.637
ΔG_C	1.919	1.205		1.931
ΔG_D	-1.421	-0.706	\†	-0.468

† "/" denotes that the adsorption of OOH on the selective active site is unstable.

Reference

(1) Rossmeisl, J.; Logadottir, A.; Lindqvist, L. *J. Phys. Chem. B*. **2004**, *108*, 1 7886–17892.

(2) Rossmeisl, J.; Logadottir, A.; Nørskov, J. K. *Chem. Phys*.**2005**, 319, 178–1 84.

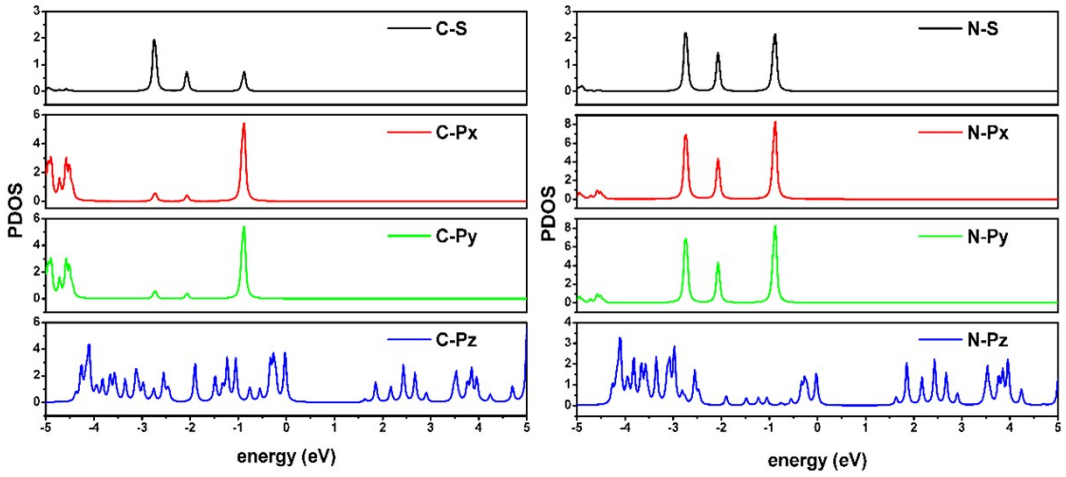

Figure S1. Partial density of states (PDOS) projected on atomic orbitals of carbon and nitrogen atoms are plotted. The Fermi energy level is set to zero.

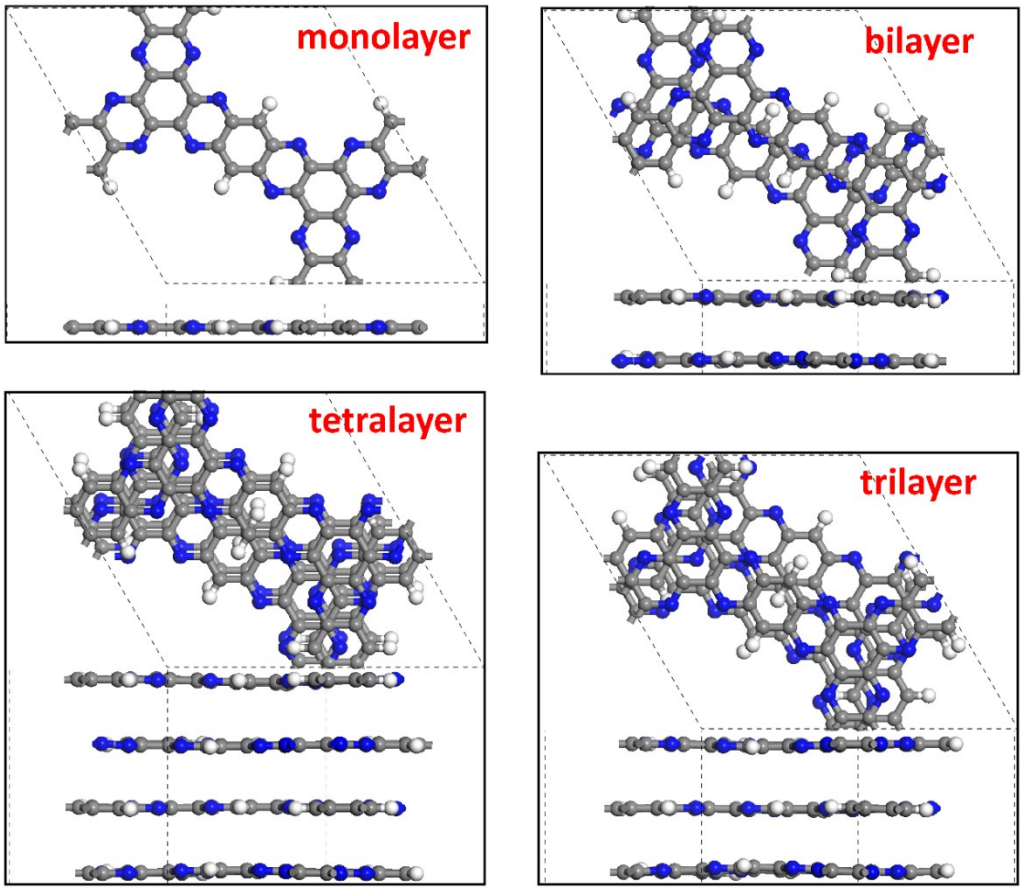

Figure S2. Top and side views of the optimized structures of aza-CMP with different number of layers.

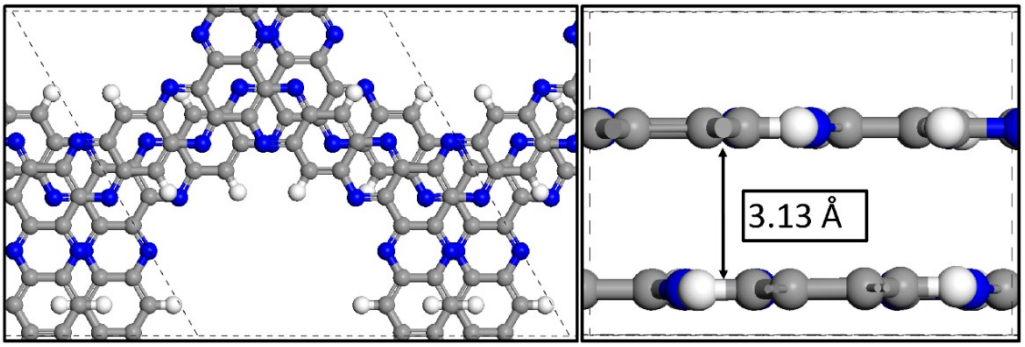

Figure S3. Top and side view of the optimized structure of bulk aza-CMP.

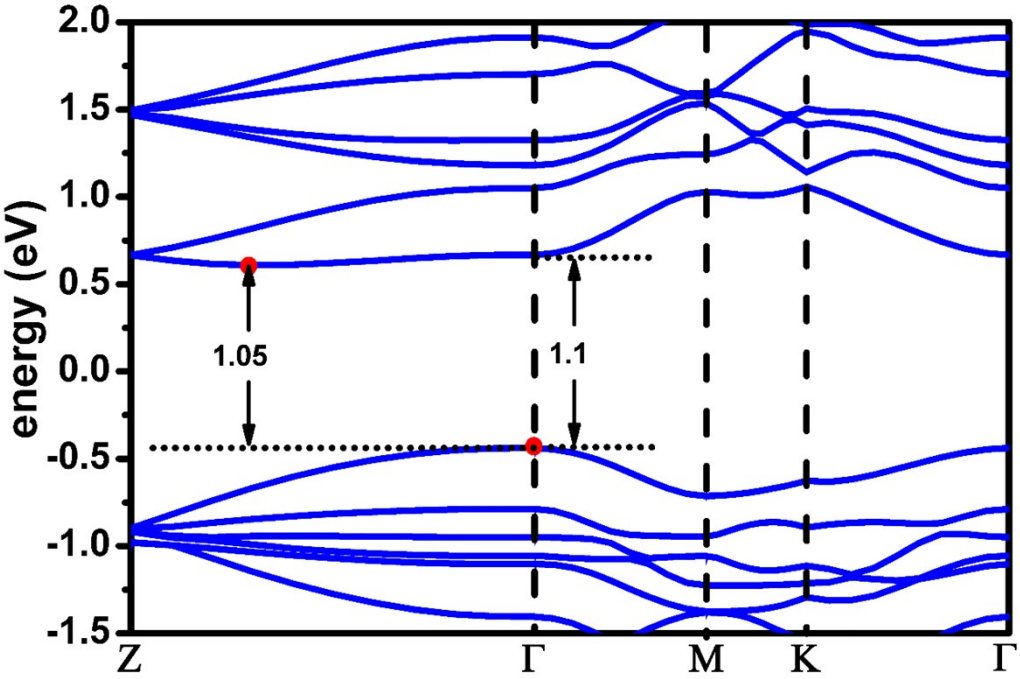

Figure S4. The calculated electronic band structure of aza-CMP bulk is plotted along high symmetry *k*-point from (0.0, 0.0, 0.5) to Γ (0.0, 0.0, 0.0), (0.0, 0.5, 0.0) and (0.333, 0.667, 0.0) in first Brillouin zone by using HSE06 method.

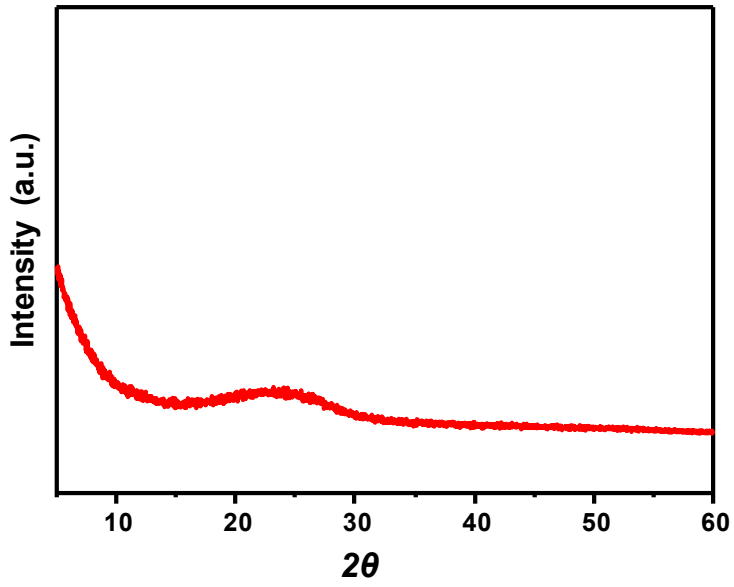

Figure S5. Powder X-ray diffraction (PXRD) pattern of as-synthesized aza-CMP. The broad peak near 27° reflects the characteristic interlayer-stacking of aromatic systems.

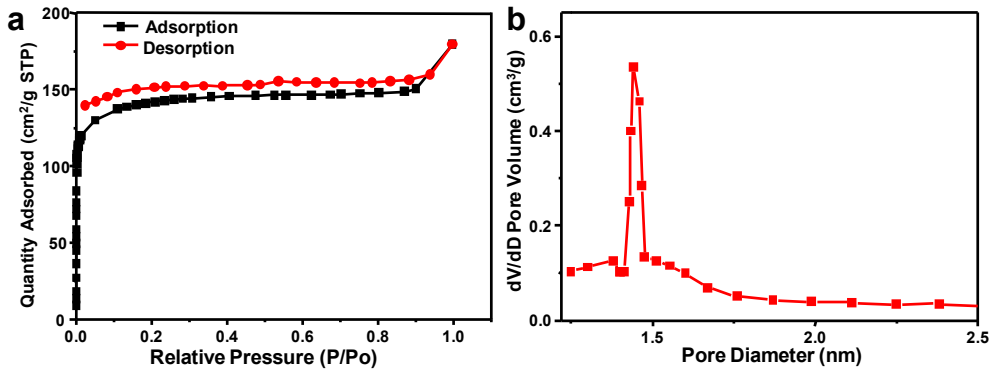

Figure S6. (a) N_2 adsorption-desorption isotherms and (b) corresponding pore size distribution of aza-CMP obtained by NLDFT method.

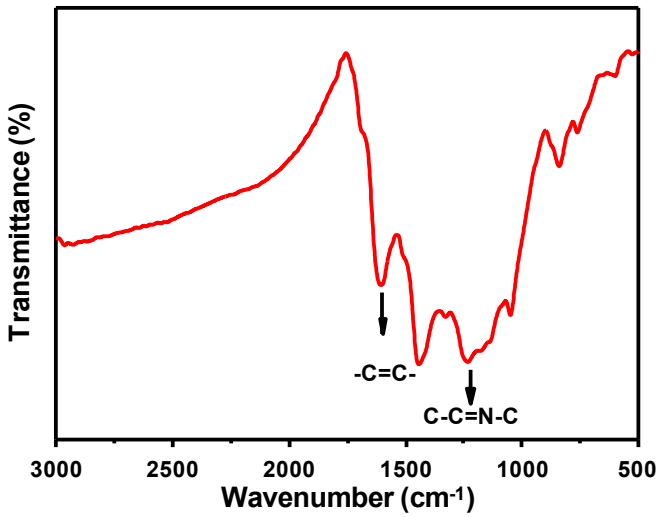

Figure S7. FTIR result of the as-synthesized aza-CMP.

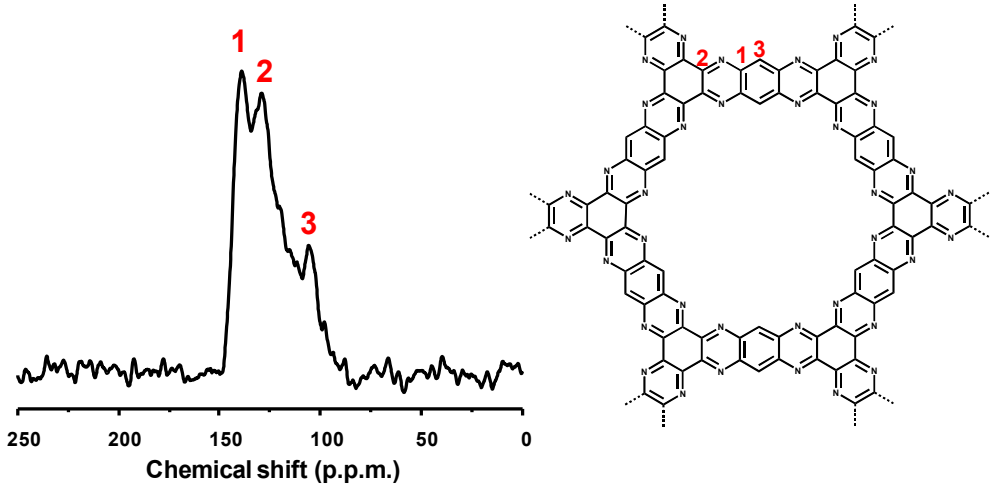

Figure S8. Solid State ^{13}C CP/MAS NMR result of aza-CMP.

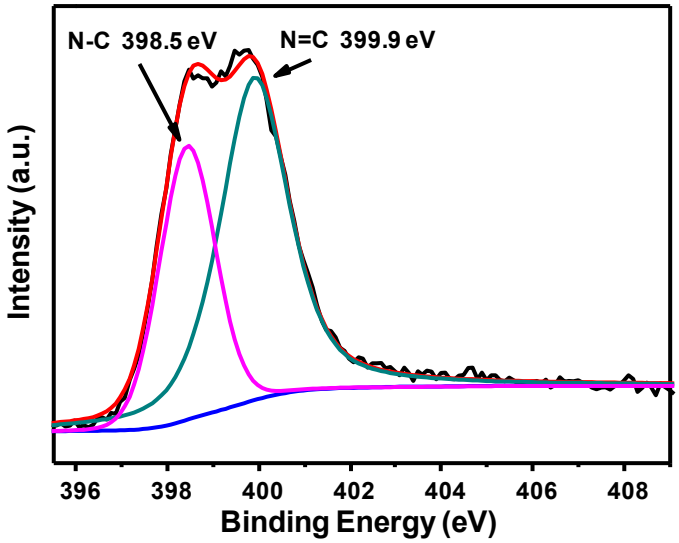

Figure S9. High resolution N 1s XPS spectrum of aza-CMP.

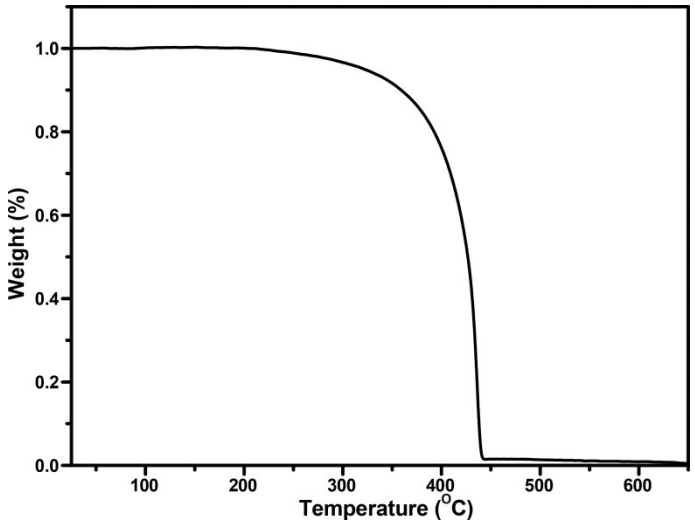

Figure S10. TGA curve of aza-CMP under air with a 10 °C/min heating rate.

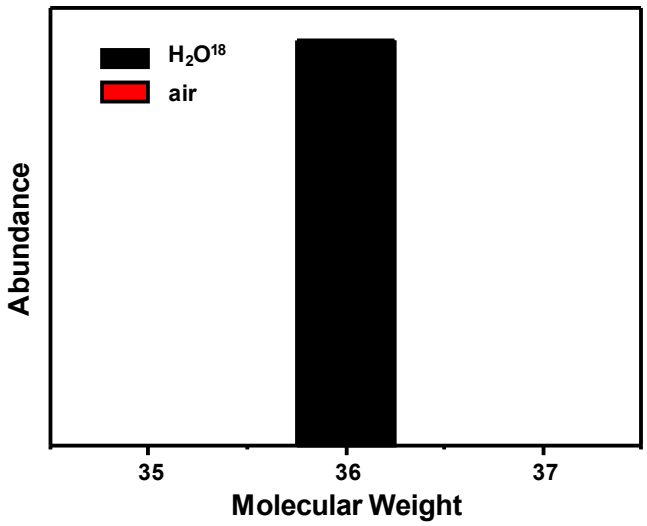

Figure S11. Representative GC-MS (an Agilent Technologies 5975C Mass Selective Detector operating in the electron impact ionization mode was used) result from $^{18}O_2$ abundance measurement via photocatalytic water oxidation using aza-CMP. Photocatalytic water splitting was performed in $H_2{}^{18}O$ to verify that O_2 was released from water splitting and not from other sources. Photocatalytically generated O_2 contains exclusively $^{18}O_2$ while no $^{18}O_2$ can be found in air. The suspension was thoroughly degassed to remove air and irradiated using a 300 W Xe lamp. A cutoff filter (Kenko L-42) was employed to achieve visible light (λ>420 nm) irradiation.

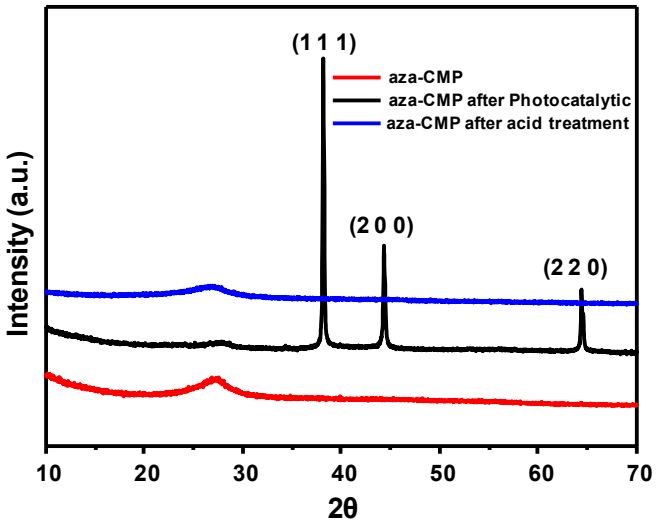

Figure S12. PXRD patterns of the aza-CMP before and after photocatalytic reactions in the presence of $AgNO_3$. After photocatalysis, Ag^+ were reduced by the photo-generated electrons and Ag nanoparticles were formed. After treatment with HNO_3, Ag nanoparticles were dissolved and the aza-CMP could recover to the pristine structure for photocatalytic O_2 evolution.

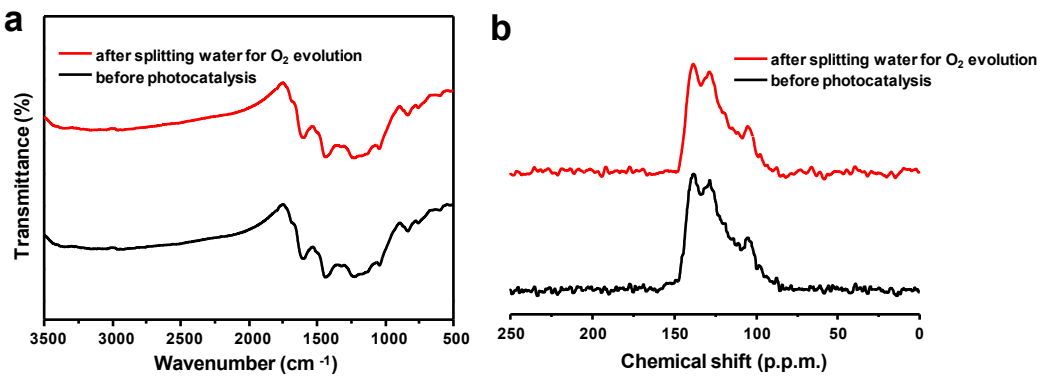

Figure S13. (a) FTIR spectra of aza-CMP before and after photocatalysis. (b) Solid-State ^{13}C CP/MAS NMR spectra of aza-CMP before and after photocatalysis. No significant changes have been observed from both characterization methods.

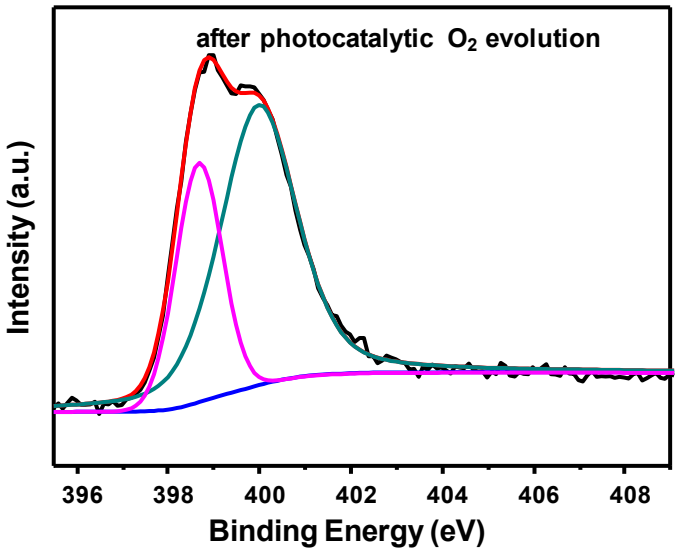

Figure S14. High resolution N 1s XPS spectra of aza-CMP after photocatalytic O_2 evolution.

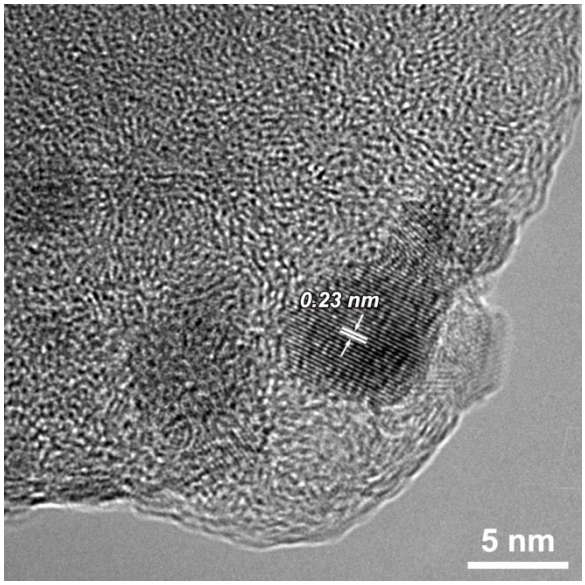

Figure S15. HRTEM image of $Co(OH)_2$/aza-CMP photocatalyst which indicates that the $Co(OH)_2$ is closed attached to the layered polymer substrate.

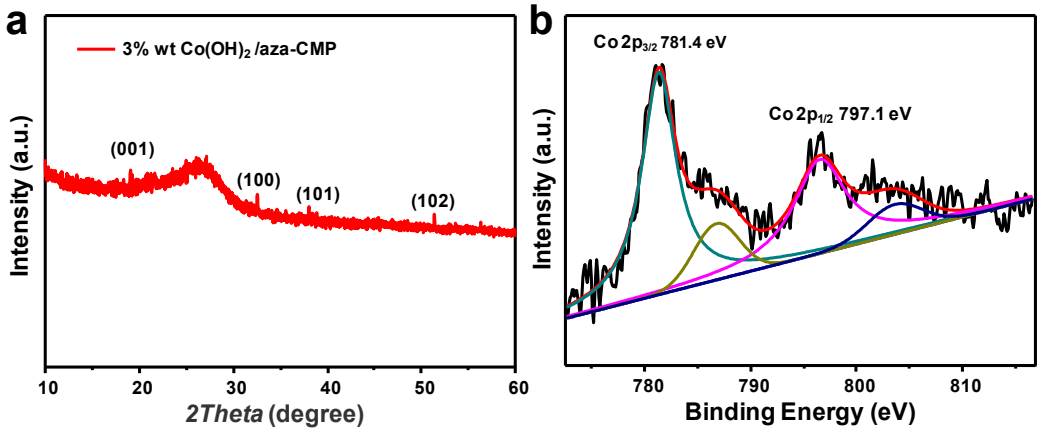

Figure S16. (a) PXRD pattern of the exfoliated aza-CMP nanosheets after deposition of $Co(OH)_2$ cocatalyst. The weak diffraction peaks are attributed to the crystalline $Co(OH)_2$ (PDF#: 30-0443). (b) High resolution Co 2p XPS spectra of aza-CMP loaded with 3 wt% $Co(OH)_2$.

Table S2. Comparison of oxygen evolution with other polymer photocatalysts without using cocatalysts under visible light irradiation.

Photocatalysts	Oxygen Evolution Rate (umol h^{-1})	Reference
exfoliated aza-CMP	3.3 (25 mg catalyst ,0.01 M $AgNO_3$)	This work
3wt% $Co(OH)_2$/ exfoliated aza-CMP	14.32 (25 mg catalyst ,0.01 M $AgNO_3$)	This work
S doped *g*-C_3N_4	2.8 (50 mg catalyst ,0.01M $AgNO_3$)	Chem. Sci. 2012, 3, 443-446.
PDINH	0.18 (50 mg, 0.1 M $AgNO_3$)	Adv. Mater. 2016,28,7294
Ni-Co LDHs/BCN-30	(50 mg catalyst ,0.01M $AgNO_3$)	nature commun 2015 6 7698
g-C_3N_4/Co-Pi	3.1 (100 mg catalyst ,0.05 M $AgNO_3$)	Appl. Catal., B 2013, 142–143, 414-422.
g-C_3N_4/Co(OH)2	7.1 (50 mg catalyst ,0.01M $AgNO_3$)	ACS Catal. 2015, 5, 941-947.
g-C_3N_4/CoSe2	9 (50 mg catalyst ,0.01M $AgNO_3$)	J. Mater. Chem. A 2015, 3, 17946-17950.
g-C_3N_4/NiFe-LDH	13.29 (30 mg catalyst ,0.03 M $AgNO_3$)	J. Mater. Chem. A 2015, 3, 18622-18635.
Co- *g*-C_3N_4	10.5 (50 mg catalyst ,0.01M $AgNO_3$)	Small 2015, 11, 1215-1221.